



NOTE

Pathology

Intermediate-grade mammary gland adenocarcinoma in an 18-year-old female black leopard (*Panthera pardus*) with acute pancreatic necrosis and chronic interstitial nephropathy

Misato NAKAMURA¹⁾, Toshinori YOSHIDA^{1)*}, Ayumi EGUCHI¹⁾, Mari INOHANA¹⁾, Rei NAGAHARA¹⁾, Ayako SHIRAKI^{1,2)}, Nanao ITO³⁾ and Makoto SHIBUTANI¹⁾

¹⁾Laboratory of Veterinary Pathology, Veterinary Science, Tokyo University of Agriculture and Technology, 3-5-8 Saiwai-cho, Fuchu-shi, Tokyo 183-8509, Japan

²⁾Pathogenetic Veterinary Science, United Graduate School of Veterinary Sciences, Gifu University, 1-1 Yanagido, Gifu-shi, Gifu 501-1193, Japan

³⁾Hirakawa Zoological Park, 5669-1 Hirakawa-cho, Kagoshima-shi, Kagoshima 891-0133, Japan

ABSTRACT. An 18-year-old female black leopard (*Panthera pardus*) showed renal failure, leukocytosis and presence of subcutaneous masses in the lower abdominal region and right shoulder; she eventually died. Histopathological observations included a mammary gland carcinoma with comedo, solid and tubulopapillary patterns in subcutaneous tissue, and highly proliferated tumor cells in systemic organs. The tumor cells were positive for cytokeratin AE1/AE3. The mammary gland tumor was diagnosed as intermediate-grade adenocarcinoma, based on a previously reported histological grading system of feline mammary carcinomas. Chronic interstitial nephritis was estimated to have been ongoing for 5 years, whilst acute necrotic pancreatitis in relation to tumor metastasis could have been the cause of death.

KEY WORDS: mammary gland tumor, nephritis, nondomestic zoo fields, pancreatitis

J. Vet. Med. Sci.

80(2): 337–340, 2018

doi: 10.1292/jvms.17-0570

Received: 21 October 2017

Accepted: 6 December 2017

Published online in J-STAGE:

19 December 2017

Mammary gland tumors have been reported in domestic zoo fields, affecting lions, tigers and leopards [2, 4, 5]. Most are highly malignant and metastasized. The most common histological type of tumors have a tubulopapillary pattern, followed by solid or cribriform patterns [2]. A comedo pattern is less common. We report the case of an 18-year-old female black leopard (*Panthera pardus*) that had a metastatic mammary gland tumor with comedo, tubulopapillary and solid patterns, associated with acute pancreatic necrosis and chronic interstitial nephropathy. We diagnosed the tumor based on a histological grading system of feline mammary carcinoma, reported by Mills *et al.* [3]. Feline mammary carcinoma is biologically aggressive and histopathologically malignant, and for the grading of the tumor, the Elston and Ellis (EE) histological grading system (also known as the Nottingham Grading System) has been widely adopted [6], although the EE system is originally established in assessment of invasive human breast cancer [1]. Mills *et al.* proposed species (feline)-specific systems by improving the prognostic values of histologic grading [3]. We hypothesized that the histologic grading system by Mills *et al.* [3] might be suitable for the invasive mammary gland carcinoma in domestic zoo fields.

A female black leopard (*Panthera pardus*) was born at a zoo in Japan in 1997, and bred pups in 2007, 2008, 2009 and 2011. Urinalysis revealed occult blood proteinuria in 2009. Similar observations, together with the observation of more severe urinary casts, were made in 2011. Blood biochemistry and hematology in 2014 revealed high levels of blood urea nitrogen (83.4 mg/dl), creatinine (5.0 mg/dl) and white blood cells ($219 \times 10^2/\mu\text{l}$). Subcutaneous masses in the lower abdominal region, trauma in the left forelimb, and/or eye and nasal discharges were observed in 2014 and 2015. During the observation, she was given antibiotics as part of her veterinary care. Her food intake decreased and she died in 2015 in a staggering and/or lateral position.

After necropsy, multiple subcutaneous masses, 3–6 mm in diameter, were found in the lower abdominal region and right shoulder (Fig. 1A). The masses were white to yellow-colored, with solid or lobular cut surfaces. Masses, less than 10 mm in diameter, were scattered in the lung, heart, liver, spleen and kidneys. In the lung, white masses were frequently observed throughout the lobes (Fig. 1B), whilst in the heart, white masses were scattered in the wall of the right ventricle (Fig. 1C).

*Correspondence to: Yoshida, T.: yoshida7@cc.tuat.ac.jp

©2018 The Japanese Society of Veterinary Science



This is an open-access article distributed under the terms of the Creative Commons Attribution Non-Commercial No Derivatives (by-nc-nd) License. (CC-BY-NC-ND 4.0: <https://creativecommons.org/licenses/by-nc-nd/4.0/>)

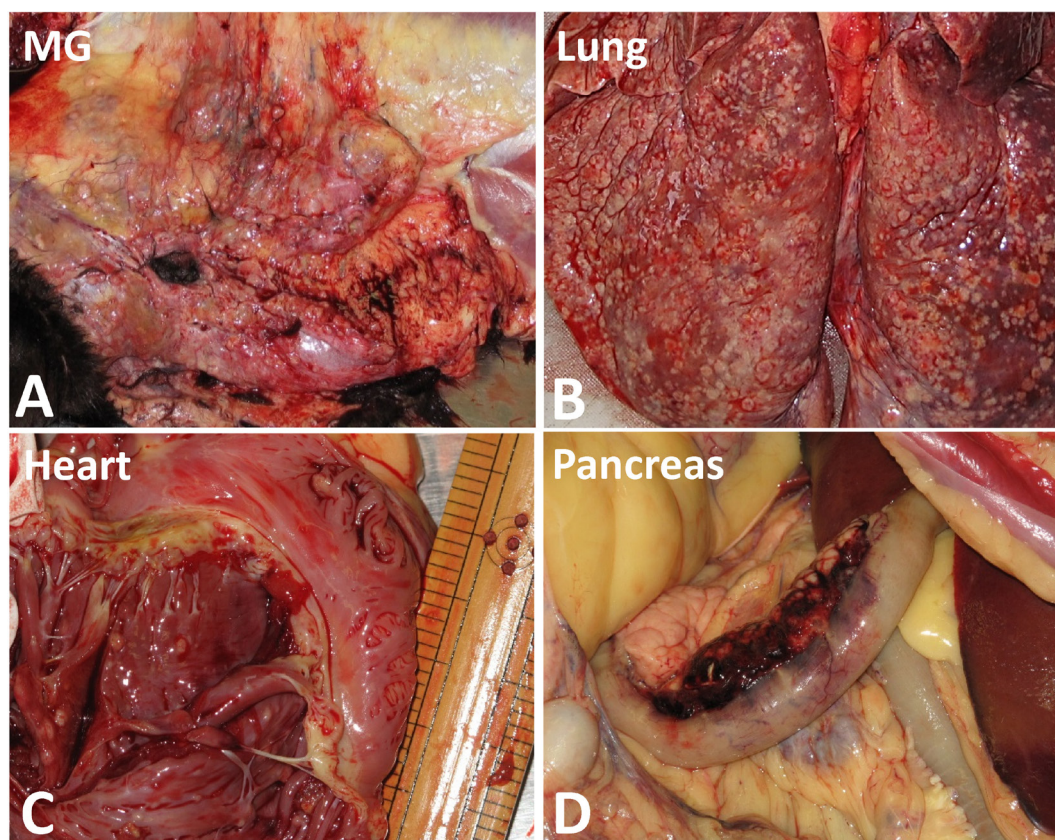


Fig. 1. Mammary gland tumors and metastatic tumors; black leopard. Yellow to pale red-colored masses were observed in the abdominal subcutaneous region (A). Multiple white-colored masses were frequently observed in lung lobes (B). White-colored masses were seen in the right ventricular wall (C). Hemorrhage was found in the pancreas and duodenum (D).

Hemorrhage was observed in the pancreas in close proximity of the duodenum (Fig. 1D). Atrophy and discoloration were found on both sides of the kidneys. These and other organs, including the salivary glands, stomach, small and large intestines, pancreas, mesenteric lymph nodes, urinary bladder, ovaries, uterus and adrenal glands, were fixed in a 10% neutral-buffered formalin, processed according to standard protocols and embedded in paraffin. Paraffin sections (5 μ m) were stained with hematoxylin and eosin. For immunohistochemical analyses, sections (subcutaneous masses, heart and kidneys) were incubated with the following primary antibodies: anti-cytokeratin AE1/AE3 (ready to use, mouse monoclonal; Dako, Glostrup, Denmark A/S), anti-vimentin (goat polyclonal, 1:200; Santa Cruz Inc., Dallas, TX, U.S.A.), and anti- α -smooth muscle actin (a-SMA; mouse monoclonal 1A4; 1:100; Dako). For antigen retrieval, deparaffinized sections were heated in: 1) 10 mM citrate buffer (pH 6.0) at 121°C in an autoclave for 10 min for AE1/AE3 detection, 2) Dako target retrieval solution (pH 9.0, Dako) at 90°C in a microwave for 10 min for a-SMA detection, and 3) 10 mM citrate buffer (pH 6.0) at 90°C in a microwave for 10 min for vimentin detection. Expression was detected using a VECTASTAIN[®] Elite ABC kit (Vector Laboratories, Inc., Burlingame, CA, U.S.A.) with 3,3'-diaminobenzidine/hydrogen peroxide as the chromogen. The sections were then counterstained with hematoxylin. For negative controls, the primary antibodies were replaced with non-immunized sera.

Variable-sized subcutaneous masses, with characteristics of mammary gland tumors, were demarcated by fibrous connective tissues and composed of tumor cells, which proliferated in mainly comedo (Fig. 2A), followed by solid (Fig. 2B) or tubulopapillary (Fig. 2C) patterns. A cribriform pattern was occasionally found. Eosinophilic secretions and cholesterol crystals were observed within tubular structures in tubulopapillary areas and necrosis at the central portion of comedo areas. The tumor cells had relatively small-sized, moderately variable shaped nuclei with prominent nucleoli, and giant nuclei were frequently observed. Mitotic counts were 9 or 10 per 10 high power field (HPF) in the solid or comedo areas, respectively. No mitotic figures were counted in the tubular areas. The tumor cells had moderate to abundant eosinophilic cytoplasm and ill-defined cell borders. Small clusters of tumor cells were observed within several lymphatic vessels in the interstitium. Atrophic normal mammary glands were observed in the surrounding tumor tissues.

In the lung, small to large proliferative lesions with irregular-shaped necrosis were scattered in lung parenchyma, and tumor cells with prominent nuclear atypia and abundant eosinophilic cytoplasm proliferated in cribriform or comedo growth patterns. Mitosis was frequently observed. Small-sized invasive lesions were frequently observed in the alveoli and vasculature (Fig. 2D). Intra-alveolar and interstitial edema were evident in the surrounding intact areas. In the heart, several variable-sized proliferative lesions with ill-defined borders were observed. The tumor cells proliferated in cribriform or comedo growth patterns, and invaded cardiac fibers. There were hemorrhagic and granulomatous tissues in subendocardial regions. In the kidneys, ill-defined proliferative lesions were scattered in the

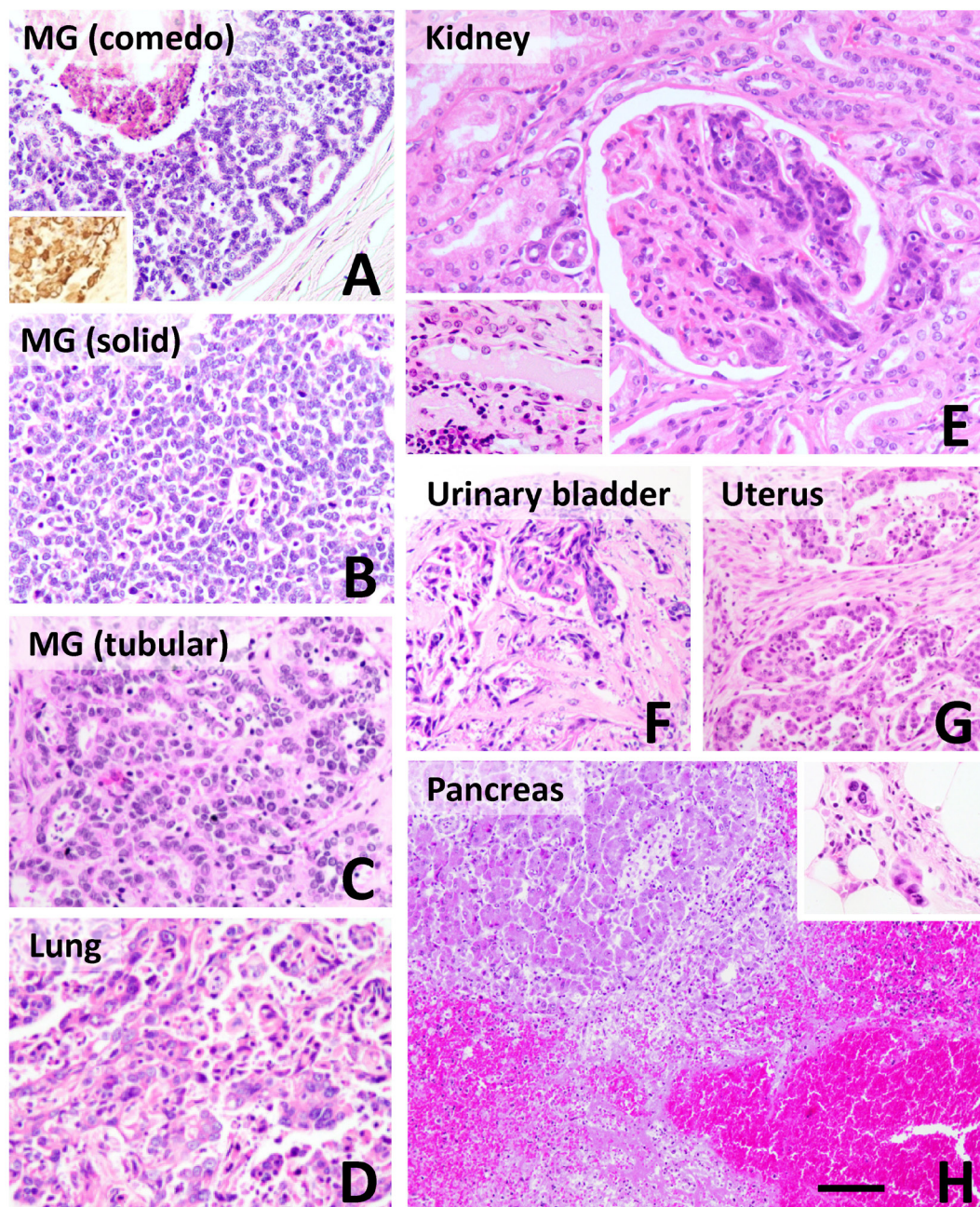


Fig. 2. Mammary gland tumors and metastatic tumors; black leopard. Mammary gland (MG) tumor cells proliferated in comedo (A), solid (B) and tubular (C) patterns. Tumor cells expressed cytokeratin AE1/AE3 (A, inset). Interstitial fibrosis was observed between tumor cells (C). In the lung, tumor cells proliferated in the alveolar walls and spaces (D). In the kidney, tumor cells infiltrated glomerulus and interstitial tissues (E). Protein cast was seen in renal tubules and mononuclear cell infiltration was seen in the interstitium (E, inset). In the urinary bladder, tumor cells metastasized to lamina propria (F). In the uterus, tumor cells proliferated in a comedo pattern between uterine leiomyoma cells (G). In the pancreas, necrosis of acinar cells along with hemorrhage was observed on the lower side (H). The tumor cells with abundant eosinophilic cytoplasm and nuclear atypia proliferated in the interstitium and capsule of pancreas (H, inset). (A–H) Hematoxylin and eosin staining. (A, inset) Immunohistochemistry; hematoxylin counterstain. Bar=50 μ m (A–G) or 100 μ m (H) (except for insets).

cortex. Tumor cells proliferated in cribriform, comedo or tubulopapillary growth patterns, and were frequently found in the capillary lumen of glomeruli and interlobular vasculatures (Fig. 2E). There was severe interstitial fibrosis with mononuclear cell infiltration, and thickening of basement membranes and protein casts in Bowman's capsules and renal tubules (Fig. 2E, inset).

Tumor cells also invaded the vasculatures and parenchymal tissues of other organs, including the liver, spleen, urinary bladder, ovaries, uterus, mesenteric lymph nodes and adrenal glands. In the urinary bladder, tumor cells with comedo or cribriform growth patterns prominently proliferated throughout the lamina propria and tunica muscularis (Fig. 2F). In the uterus, tumor

cells invaded leiomyomatous tissue, with well-differentiated spindle shaped cells with intersecting fascicles that protruded into the lumen (Fig. 2G). In the mesenteric lymph nodes, tumor cells proliferated in lymphatic sinuses, and invaded the surrounding intraabdominal adipose tissues, with evidence of cancerous peritonitis. In the pancreas, massive hemorrhaging, necrosis and inflammatory cell infiltration (mainly neutrophilic) were observed (Fig. 2H), and local atrophy of acinar cells and interstitial fibroses were also noted. A small number of tumor cells invaded interstitium (Fig. 2H, inset) and capsule. Necrosis, hemorrhage, inflammatory cell infiltration and tumor cell invasion were observed in surrounding abdominal tissues and duodenum (submucosal tissues to serosa) that was close to the pancreas. No abnormalities were detected in the salivary gland, stomach or large intestines.

Immunohistochemically, the epithelial tumor cells in the mammary gland were positive for cytokeratin AE1/AE3 (Fig. 2A, inset), and negative for α -SMA and vimentin. The metastatic tumor cells in the heart and kidneys showed similar positive reactions.

The present case was suspected to be derived from the mammary gland, because normal mammary gland was observed in the vicinity of tumor tissues. The subcutaneous masses in the lower abdominal region might be the primary lesion, while those in the right shoulder and masses in other organs could be metastatic lesions. The mammary gland tumors were initially diagnosed as intermediate or moderately differentiated mammary carcinomas, based on the EE histological grading system [1]. According to their criteria, scores for tubular formation, nuclear pleomorphism and mitosis per 10 HPF were 2 (10–75%), 2 (moderately increased) and 2 (9–16 mitotic cells per 10 HPF), respectively, with a total score of 6 (intermediate or moderately differentiated). Mills *et al.* proposed a novel grading system using lymphovascular invasion, nuclear form and mitotic counts, as the EE grading system fails to have a significant correlation with overall survival [3]. Mitotic counts by EE were grouped as score 1 (0–8 per 10 HPF), score 2 (9–16 per 10 HPF) and score 3 (≥ 17 per 10HPF), while those by Mills *et al.* were grouped as score 1 (≤ 62 per 10HPF) and score 2 (> 62 per 10HPF) [3]. Nuclear pleomorphism scoring by EE includes score 1 (small, regular, uniform nuclei), 2 (nuclei with moderately increased size, vesiculation and variability) and 3 (nuclei with vesicular chromatin and marked variation in size), while nuclear form scoring by Mills *et al.* includes score 0 (less than 5% abnormal nuclei) and score 1 (more than 5% abnormal nuclei) [3]. According to the Mills *et al.* grading system [3], the tumor may have been a grade II (intermediate-grade) carcinoma, as scores for lymphovascular invasion, nuclear form and mitotic count were 1, 0 ($< 5\%$ abnormal) and 0 (> 62 per 10 HPF), respectively, and the total score was 1 (grade II). Grading this as an intermediate-grade carcinoma might be appropriate, considering the histological grading by Mills *et al.* [3] as well as EE [1]. Mammary cystadenoma was reported in one leopard (*Panthera pardus*) [4]; however, mammary carcinoma has not been reported to our knowledge. As no reports using histological grading systems on feline mammary adenocarcinoma are available in zoo fields, further studies are required to confirm whether our preliminary investigation was appropriate. The present case should be considered spontaneous, as medical treatment with melengestrol acetate, a potent synthetic progestin contraceptive, which might be associated with the tumor development [2], has never been conducted.

The present case had chronic interstitial nephritis and acute pancreatic necrosis. Chronic interstitial nephritis was estimated to have been present for 5 years, characterized by prominent interstitial fibrosis throughout the cortex to the medulla. Chronic renal disease with unknown etiology is the most concurrent disease in captive lions with mammary gland tumors [5]. Tumor metastasis in the kidneys might result in worse clinical outcomes. Pancreatitis is the most common disorder of the exocrine pancreas in cats, and is clinically important in this species [7], but is not reported in detail in domestic zoo fields to our knowledge. Classification of feline pancreatitis has not been universally standardized; however, it may be classified into acute necrotic pancreatitis, acute suppurative pancreatitis and chronic pancreatitis [7]. The present pancreatic lesion was diagnosed as acute necrotic pancreatitis, with wide-spread necrosis including pancreatic acinar cell and/or peripancreatic fat necrosis. Several viral and parasitic agents have been shown or suspected to be occasionally associated with cases of feline pancreatitis [7]; however evidence of infection was not demonstrated in the present case. Pancreatic ductal obstruction caused by tumor metastasis might be also key to the development of pancreatic necrosis [7]. Thus, acute pancreatic necrosis lesions presumably secondary to tumor metastasis may have been the cause of death in the present case.

The present case provides evidence of intermediate-grade mammary gland carcinoma, and the feline mammary carcinoma grading system, proposed by Mills *et al.* [3], may be adopted to assess in tumors in zoo fields.

ACKNOWLEDGMENT. The authors thank Mrs. Shigeko Suzuki for her technical assistance in preparing the histological specimens.

REFERENCES

1. Elston, C. W. and Ellis, I. O. 1991. Pathological prognostic factors in breast cancer. I. The value of histological grade in breast cancer: experience from a large study with long-term follow-up. *Histopathology* **19**: 403–410. [Medline] [CrossRef]
2. McAloose, D., Munson, L. and Naydan, D. K. 2007. Histologic features of mammary carcinomas in zoo felids treated with melengestrol acetate (MGA) contraceptives. *Vet. Pathol.* **44**: 320–326. [Medline] [CrossRef]
3. Mills, S. W., Musil, K. M., Davies, J. L., Hendrick, S., Duncan, C., Jackson, M. L., Kidney, B., Philibert, H., Wobeser, B. K. and Simko, E. 2015. Prognostic value of histologic grading for feline mammary carcinoma: a retrospective survival analysis. *Vet. Pathol.* **52**: 238–249. [Medline] [CrossRef]
4. Owston, M. A., Ramsay, E. C. and Rotstein, D. S. 2008. Neoplasia in felids at the Knoxville Zoological Gardens, 1979–2003. *J. Zoo Wildl. Med.* **39**: 608–613. [Medline] [CrossRef]
5. Sadler, R. A., Craig, L. E., Ramsay, E. C., Helmick, K., Collins, D. and Garner, M. M. 2016. Clinicopathologic features of mammary masses in captive lions (*Panthera Leo*). *J. Zoo Wildl. Med.* **47**: 127–131. [Medline] [CrossRef]
6. Seixas, F., Palmeira, C., Pires, M. A., Bento, M. J. and Lopes, C. 2011. Grade is an independent prognostic factor for feline mammary carcinomas: a clinicopathological and survival analysis. *Vet. J.* **187**: 65–71. [Medline] [CrossRef]
7. Xenoulis, P. G. and Steiner, J. M. 2008. Current concepts in feline pancreatitis. *Top. Companion Anim. Med.* **23**: 185–192. [Medline] [CrossRef]